Electronic Supplementary Information (ESI)

Organic and perovskite solar modules innovated by adhesive top electrode and depth-resolved laser patterning

George D. Spyropoulos[1]*, César Omar Ramirez Quiroz[2], Michael Salvador[2,5], Yi Hou[2,4], Nicola Gasparini[2], Peter Schweizer[3], Jens Adams[1], Peter Kubis[1,4], Ning Li[2], Erdmann Spiecker[3], Tayebeh Ameri[2], Hans-Joachim Egelhaaf[1] and Christoph J. Brabec[1,2]

Table S1. Power conversion efficiencies of laminated organic solar cells due date

	PCE (%)
J. Huang et al. 2008[1]	3.00
B. A. Bailey et al. 2011[2]	3.19
Y. Yuan et al. 2011[3]	4.00
C. Shimada et al. 2013[4]	2.41
D. Kaduwal et al. 2014[5]	2.50
R. Steim et al. 2015[6]	1.60
Current work	5.88

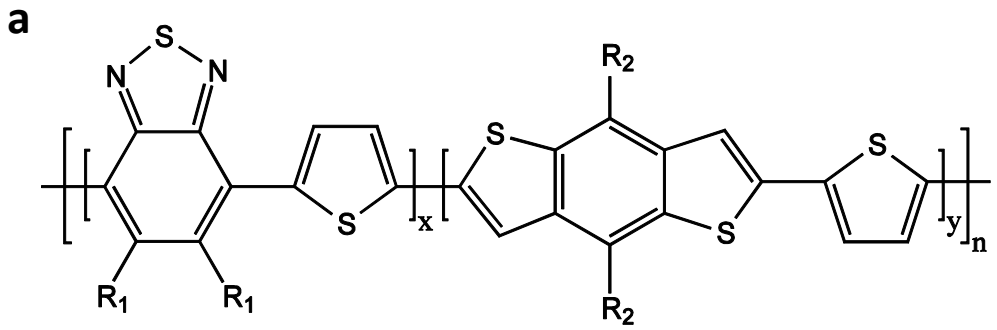

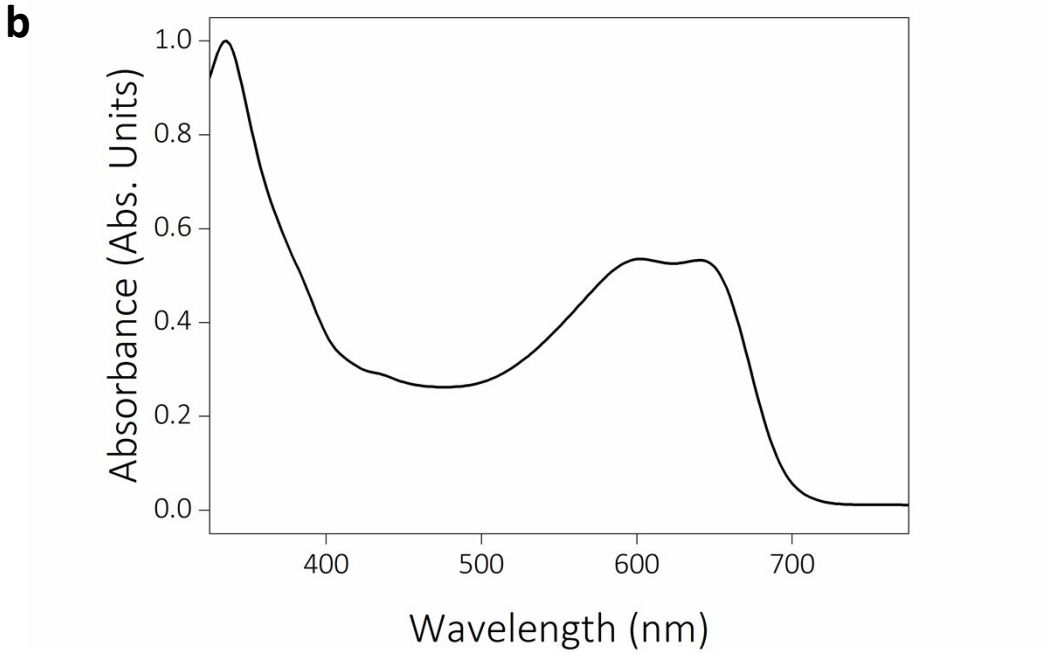

Figure S1. a) Chemical structure of PBTZT-stat-BDTT-8[7]. **b)** UV-VIS absorption spectrum of PBTZT-stat-BDTT-8 : PC[60]BM film.

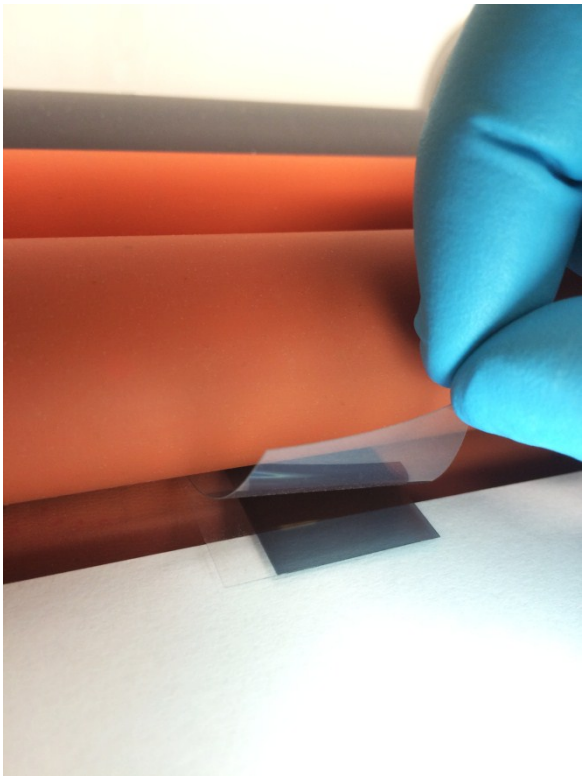

Figure S2. Photograph of the lamination process. The two substrates bearing the active layers and the top contact are driven through a pre-heated (120 °C) roll laminator consisting of three rolls for intimate electrical contact.

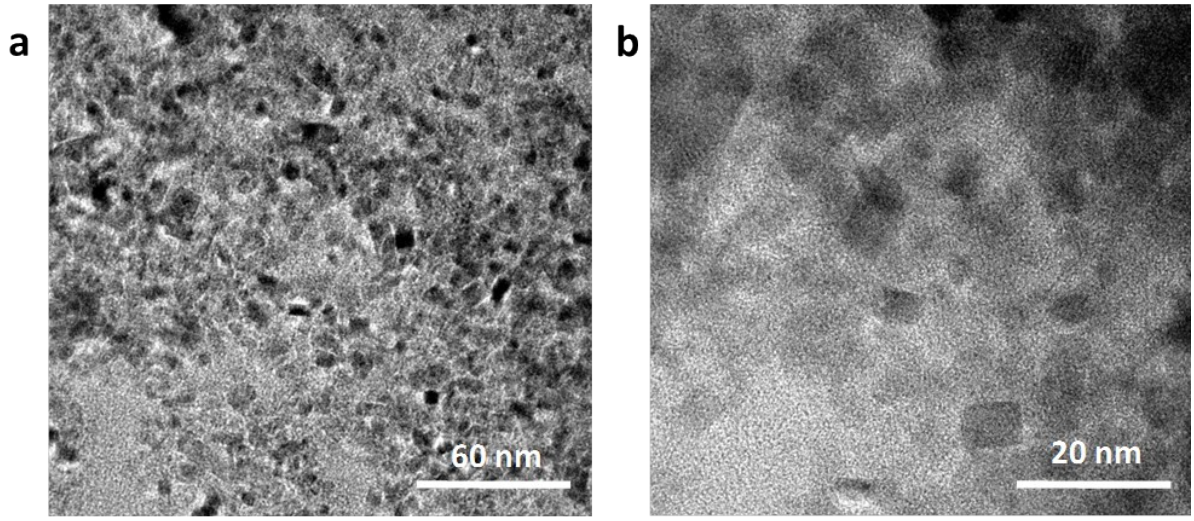

Figure S3. a) Low magnification bright-field transmission electron microscopy image of NiO nanoparticles. **b**) High magnification bright-field transmission electron microscopy image of NiO nanoparticles.

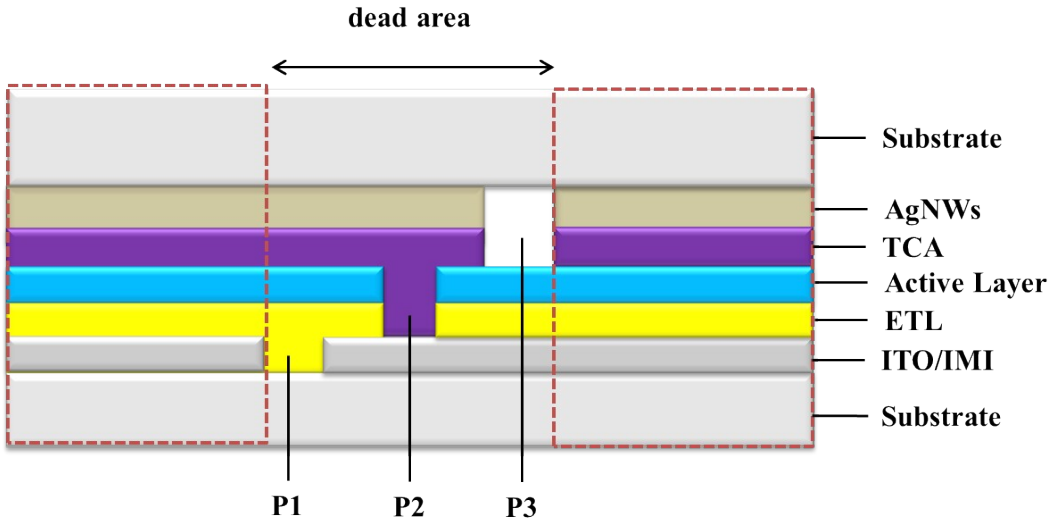

Figure S4. The P1 and P2 line are scribed before the lamination process while the P3 line is post-patterned through the top substrate.

Table S2. Jsc values of each device calculated from PCE spectra shown in Fig,2g and Fig, 4d

	Electrode/Measurement	J_{sc} calculated from EQE spectra (mA/cm^2)
PBTZT-stat-BDTT-8:PCBM cell	Evaporated Ag	12.67
PBTZT-stat-BDTT-8:PCBM cell	Laminated/ wo mirror	11.02
PBTZT-stat-BDTT-8:PCBM cell	Laminated/ with mirror	12.08
$CH_3NH_3PbI_3$ cell	Evaporated Ag	18.21
$CH_3NH_3PbI_3$ cell	Laminated/ wo mirror	14.94
$CH_3NH_3PbI_3$ cell	Laminated/ with mirror	16.18

a

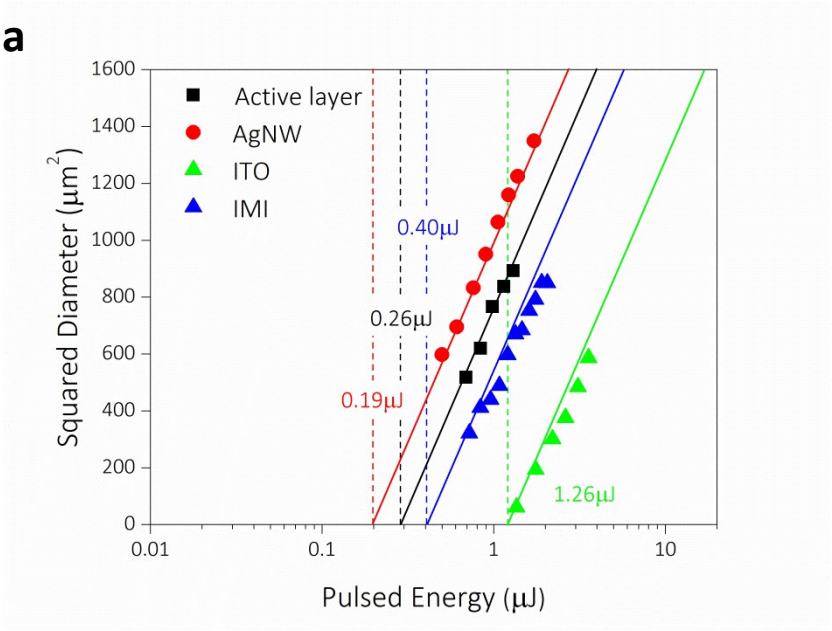

b

Material	Threshold fluence (J/cm²)
IMI	0.1
AgNW	0.04
ITO	0.29
Active Layer	0.08

Figure S5. a) Squared Diameter of ablated area versus laser pulsed energy. **b**) Calculated threshold fluence for each functional film[8, 9]. The difference in threshold fluence allows to successively scribing interconnection lines w/o damaging other active layers of the device stack. Active layer refers to the organic absorber. The ablation threshold of perovskite based active layer is generally similar to organic or even slightly higher.

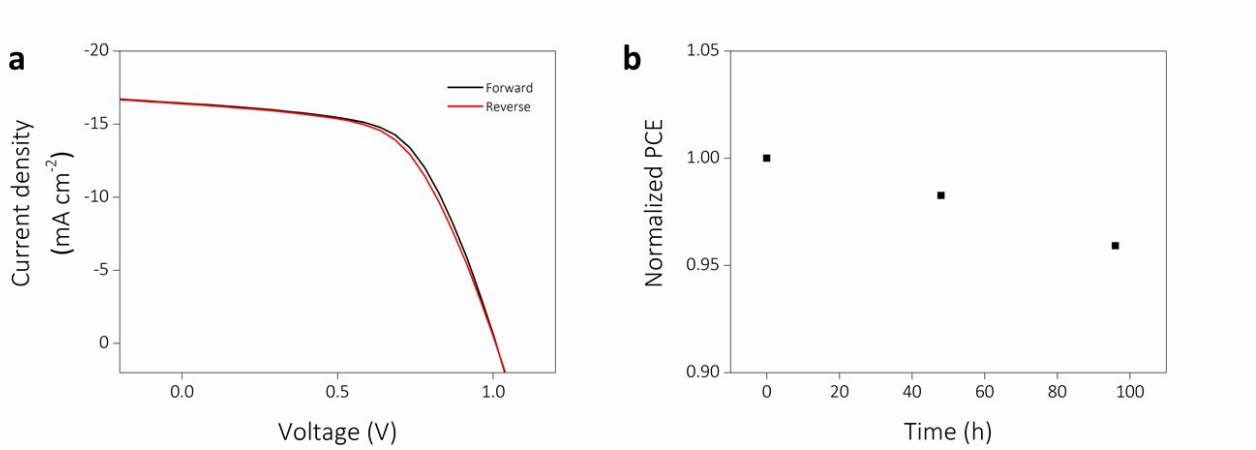

Figure S6. a) J-V characteristics of representative perovskite solar cell with laminated top electrode measured under forward (black line) and reverse (red line) bias scanning. **b**) Change in PCE of a perovskite solar cell with laminated top electrode over ≈100 h (stored in N_2).

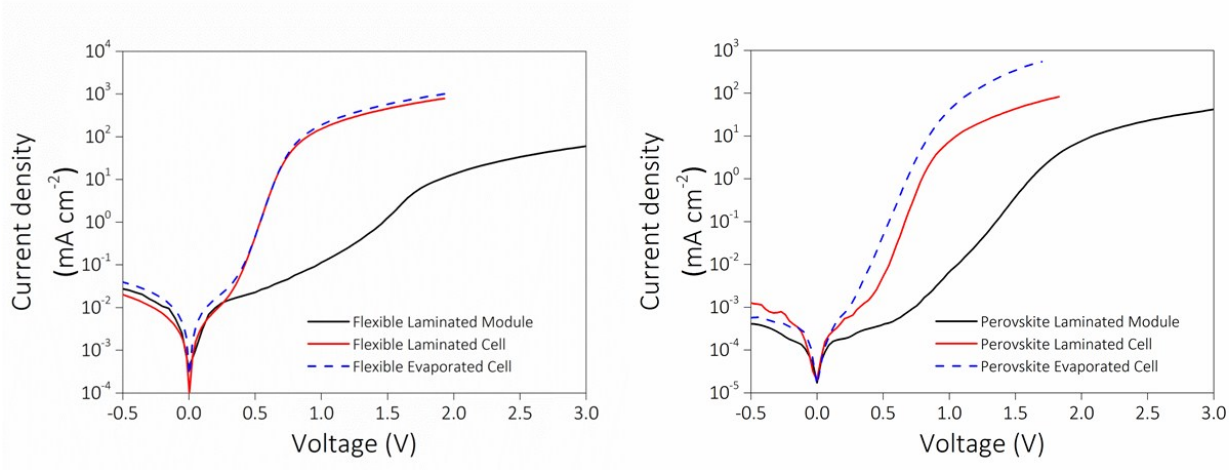

Figure S7. a) J-V characteristics under dark conditions for flexible OPV devices with laminated and evaporated top electrode. **b)** J-V characteristics under dark conditions for perovskite devices with laminated and evaporated top electrode

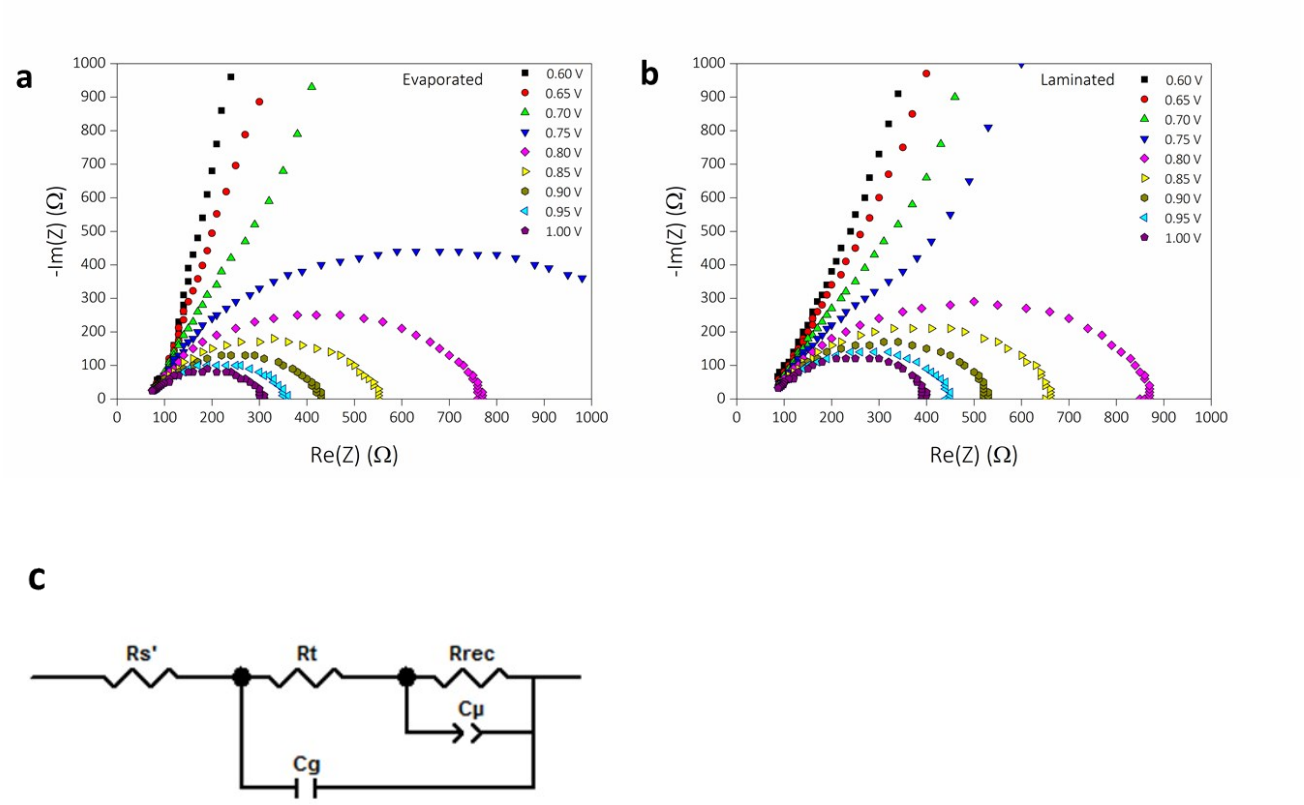

Figure S8. a) Impedance spectra for devices with evaporated top electrode under different applied biases. **b)** Impedance spectra for devices with laminated top electrode under different applied biases. EIS Spectrum Analyser was used for analysis and simulation of impedance spectra[10]. **c)** Equivalent circuit used for fitting data obtained by impedance spectroscopy. C_g and C_μ represent geometrical and chemical capacitance, respectively.. R_{rec} denotes the recombination resistance and R_t represents the transport resistance. R_s' denotes an additional resistive element due to electrode resistance losses.. For applied biases greater than V_{oc} the total series resistance in the model is given by $R_s = R_s' + R_t$

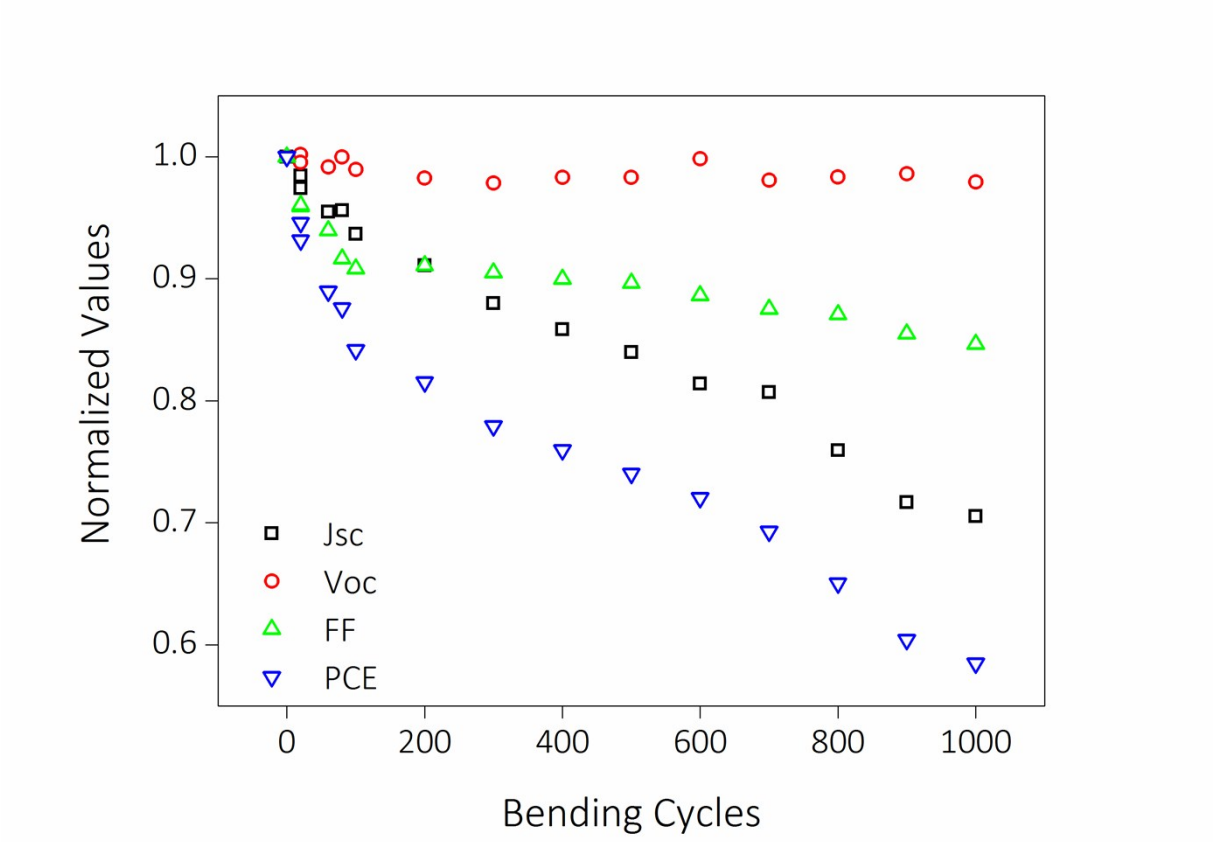

Figure S9. Normalized device characteristics of a flexible organic laminated solar cell over successive bending cycles.

References

1. J. Huang, G. Li and Y. Yang, *Adv. Mater.*, 2008, **20**, 415-419.
2. B. A. Bailey, M. O. Reese, D. C. Olson, S. E. Shaheen and N. Kopidakis, *Org. Electron.*, 2011, **12**, 108-112.
3. Y. Yuan, Y. Bi and J. Huang, *Appl. Phys. Lett.*, 2011, **98**, 063306.
4. C. Shimada and S. Shiratori, *ACS Appl. Mater. Interfaces*, 2013, **5**, 11087-11092.
5. D. Kaduwal, B. Zimmermann and U. Würfel, *Sol. Energy Mater. Sol. Cells*, 2014, **120, Part B**, 449-453.
6. R. Steim, P. Chabrecek, U. Sonderegger, B. Kindle-Hasse, W. Siefert, T. Kroyer, P. Reinecke, T. Lanz, T. Geiger, R. Hany and F. Nüesch, *Appl. Phys. Lett.*, 2015, **106**, 193301.
7. S. Berny, N. Blouin, A. Distler, H.-J. Egelhaaf, M. Krompiec, A. Lohr, O. R. Lozman, G. E. Morse, L. Nanson, A. Pron, T. Sauermann, N. Seidler, S. Tierney, P. Tiwana, M. Wagner and H. Wilson, *Advanced Science*, 2015, DOI:10.1002/advs.201500342.
8. J. M. Liu, *Opt. Lett.*, 1982, **7**, 196-198.
9. A. Ben-Yakar and R. L. Byer, *J. Appl. Phys.*, 2004, **96**, 5316-5323.
10. G. A. Ragoisha and A. S. Bondarenko, *Electrochimica Acta*, 2005, **50**, 1553-1563.